Shake Table Testing and Analysis of Two-Column Bents

David Sanders[1], Khaled Moustafa[2], M. Saiid Saiidi[1], Saad El-Azazy[3]

1) University of Nevada, Reno, Nevada 89502
2) Saiful/Bouquet Structural Engineers, Pasadena, CA 91101
3) Program Manager, California Department of Transportation, Sacramento, CA

INTRODUCTION

Structural design of bridge components, such as columns, beam-column joints, and cap beams has evolved in the past 20 years. Most of the tests conducted to develop design procedures were static performed by monotonic cyclic loadings. Therefore, this study investigated the seismic behavior of the models of the two-column bridge bents by subjecting them to dynamic earthquake motions. The study also aimed to model the actual bridge mass to have more realistic representation of dynamic mass and the P-δ effect. Based on the 0.3-scale model developed from a previous study [2], three specimens were designed using Caltrans specifications [1] and recommendations. The design focused on column confinement, column shear capacity, and the seismic details of the longitudinal and transverse reinforcement in the cap beam and in the beam-column joint. The three specimens were identical except for the column aspect ratios, which were 2.5, 4.5, and 6.64.

SPECIMEN DESIGN AND TEST SETUP

The design configuration for the three specimens is shown in Fig. 1. Several computer programs were used to predict the seismic behavior of the test specimens and to ensure that all specimens would reach total failure before exceeding the maximum shake table capacity. Using the expected seismic behavior obtained from computer analysis, an instrumentation layout was designed to measure specimen acceleration and displacement and to record concrete and steel strains generated during testing.

Lead weight was used to simulate the weight of the structure. To produce realistic stresses in the columns and beam, the amount of lead was set such that an axial load in each column of 0.05 $f'_c A_g$ was created where f'_c is the concrete compressive strength and A_g is the column gross area. Steel buckets were designed to contain the lead blocks and be attached on the cap beam of each specimen. Fig. 2 shows the lead buckets placed on middle height specimen. The loading system allowed the mass on each bent to move freely back and forth during shaking, and it was expected for the mass to cause large displacements after forming the mechanism. Cables connected between cap beams and footings were used to restrain the specimen against total collapse. An additional steel frame was designed and attached to the shake table to secure the area around the

table and to prevent any damage to the shake table. Fig. 2 shows the stability system for the medium height specimen. The height of the horizontal beam was adjusted for each specimen.

EXPERIMENTAL RESULTS

Each specimen was loaded with increasing values of the Sylmar record from the 1994 Northridge Earthquake in California. Table 1 shows the sequence of loadings for each specimen. The input acceleration for 1.0 x Sylmar was 0.61g. The earthquake time step was scaled with a factor equal to the square root of the model scaling factor to enable the same seismic response of the model as the prototype subjected to the same earthquake. The acceleration level of the earthquake was multiplied by a factor until the response reached the predicted maximum displacement. The duration of the earthquake was not changed as the record was multiplied. The load-displacement cumulative hysteresis curves for the three specimens are shown in Fig. 3. The increase in specimen maximum displacement and the reduction in the specimen lateral capacity are evident as the specimen aspect ratio increases from 2.5 to 6.64 (from short to tall specimens, respectively). Table 2 provides a summary of the experimental results. In the short specimen, the failure mode was a mixture of flexural and shear. This was clearly shown in column flexural and shear cracks. Fig 4 shows a short specimen column after the maximum load (3.25 x Sylmar). In the plastic hinge zones of both columns, concrete spalled till exposing the column spiral. The concrete started to spall at the loading of 2.5 x Sylmar and the column longitudinal reinforcement started to yield during the loading of 1.75 x Sylmar. The test was stopped due to failure at the column base. During the maximum loading, the maximum reported base displacement was 0.5" at the east column base. There was no spalling in the east column base because of the low column compression since the predominant motion of Sylmar record is in the west direction of the specimen. The compression failure at the base was as a result of the lack of confinement in this region and the large compression force.

In the medium and tall specimens, the failure mode was primarily flexural. As shown in Fig. 5, the maximum loading caused deep concrete spalling till exposing the longitudinal and transverse reinforcement in the expected plastic hinge zones. In the tall and medium specimens, a large piece of concrete spalled from the hinge base on the west side of the west column base. This failure was also observed in the short specimen at the same location (as mentioned earlier). Similar to the short specimen, the beam-column joints in the tall and medium specimens experienced only limited cracking.

SPECIMEN MODELING AND ANALYTICAL RESULTS

Two analytical models were used to analyze the three specimens statically and dynamically. First, each specimen was modeled with 2D-beam elements, and the system nonlinearity was represented by a lumped plasticity model. This representation was used to perform the nonlinear static (push-over) and dynamic analyses on the three specimens. The SAP2000 program [3] was used to perform the push-over analysis while the DRAIN-3DX program [4] was used to perform the dynamic analysis. The lumped plasticity model required the calculation of moment-rotation at expected plastic hinges. Reinforcement slippage was calculated and included in the model in the form of additional rotation at the expected plastic hinges. The maximum shear deformations were also included by using the column shear area after cracking. The concrete shear area for the circular columns was developed based on the truss mechanism. It was also successfully used in predicting the column shear deformation in a previous study by Laplace [5]. The push-over

analysis proved to have a good prediction for the specimen peak displacement and capacity. The details of the analytical work are illustrated in a report by Moustafa et al [6].

The strut-and-tie model was also used to predict the specimen capacity and to interpret the behavior at the specimen D-regions, e.g., beam-column joints, hinge bases and plastic hinge zones. In both models, the effect of dynamic loading on the concrete and steel properties, so called the strain rate effect, was included. In the strut-and-tie model, equilibrium was maintained between external and internal forces. As shown in Fig. 6 the external loading carried by each specimen was distributed along the specimen cap beam since the cap beam carries the dynamic mass. As a first trial, the value of the external force was taken as the total shear demand when the column critical sections reach their flexural capacities. The yielding flexural capacities of the column top and bottom sections were calculated using the RCMC program [7]. The ACI- 318 code method [8] was followed in developing the strut-and-tie model. The specimen B- and D-regions were determined as shown in Fig. 6. The flexural forces at the end of the B-regions in specimen columns were determined using the RCMC program. The axial forces in each column were calculated from the specimen equilibrium when column top and bottom sections reach their flexural yielding. After several trials, the strut-and-tie model of each specimen was selected and the final member forces were calculated. The use of strut-and-tie model showed good agreement with the experimental results [6] and provided an understanding of the behavior of the beam-column joints and hinge base regions.

CONCLUSIONS

Based on the experimental observations and analytical studies for the three specimens, the following conclusions were drawn:

- The tall and medium specimens behaved satisfactorily as their behavior was controlled by flexure whereas the short specimen behaved with combined flexure/shear mode. The short specimen failed at a lower ductility level in part due to the low performance of the base hinge.
- Sliding failure at the short column bases precluded the columns from reaching their maximum flexural capacity. Improved details are needed for base hinges.
- In all specimens, flexural concrete spalling was well contained and the column-confined core was almost intact during high levels of loadings.
- In all specimens, the cap beam experienced limited cracking.
- Despite the simplicity of the beam-column joint details, they were sufficient to protect the joints from failure. In the three specimens, measured and observed results assured that the joint strength was significantly higher than the adjoining columns.
- Using simple analytical models (2D-beam with a lumped plasticity model) in SAP2000 program showed good correlation with the experimental results.
- Using the Takeda model in DRAIN-3DX program accurately predicted the nonlinear response of the flexurally dominated specimens. For the short specimen, however, shear models need to be included in the DRAIN-3DX models to produce good behavior prediction.
- Strut-and-tie models
    - Can be used to design the beam-column joints with a more consistent way than in the principal stress method.

- Can be used as a conservative solution to determine the structure capacity and base hinge capacity in conjunction with a modified shear friction model.

- Values for strut and node capacity from the ACI 318-02 worked well in predicting behavior patterns observed.

REFERENCES

1. Caltrans Seismic Design Criteria, Version 1.1, July-1999
2. Moore, J., D.H. Sanders and M.S. Saiidi, "Shake Table Testing of Two-Column Bents with Hinged Bases", Civil Engineering. Department, University of Nevada, Reno, Report No. CCEER-99-13, August 1999.
3. SAP2000, Integrated Structural Analysis and Design Software.
4. Prakash, V., G.H. Powell, and S. Cambell, "DRAIN-3DX: Base Program User Guide, V1.1", Structural Engineering Mechanics and Materials, Department of Civil Engineering, University of California, Berkely, November 1993.
5. Laplace, P., D.H. Sanders, M.S Saiidi, and B.M. Douglas, "Experimental Study and Analysis of Refrofitted Flexure and Shear Dominated Circular Reinforced Concrete Bridge Columns Subjected to Shake Table Excitation", Civil Engineering Department, University of Nevada, Reno, Report No. CCEER-01-6, June 2001.
6. Moustafa, K., D.H. Sanders and M.S. Saiidi, "Impact of Aspect Ratio on Two-Column Bent Seismic Performance", Civil Engineering Department, university of Nevada, Reno, Report No. CCEER 04-03, May 2004.
7. Wehbe, N., and M.S. Saiidi, "User's Manual for RCMC v1.2-A Computer Program for Moment-Curvature Analysis of confined and Unconfined Concrete Sections", Civil Engineering Department, University of Nevada, Reno, Report No. CCEER-99-6, May 1999.
8. ACI 318 (2002): Building Code Requirements for Structural Concrete and Commentary. American Concrete Institute, Farmington Hills, 2002

Table 1: Testing Sequence for Three Specimens

Short Specimen		Medium Specimen		Tall Specimen	
Run	Times x Sylmar	Run	Times x Sylmar	Run	Times x Sylmar
2	0.20	2	0.10	2	0.10
3	0.25	3	0.20	3	0.20
4	0.50	4	0.25	4	0.25
5	0.75	5	0.50	5	0.50
6	1.00	6	0.75	6	0.75
7	1.25	7	1.00	7	0.85
8	1.40	8	1.25	8	1.00
9	1.75	9	1.40	9	1.25
10	2.00	10	1.50	10	1.50
11	2.125	11	1.75	11	1.75
12	2.25	12	2.00	12	2.00
13	2.375	13	2.25	13	2.25
14	2.50	14	2.50	14	2.50
15	2.625	15	2.75	15	2.75
16	2.75	16	3.00	16	
17	3.00				
18	3.25				

Table 2: Summary

Specimen	Column Concrete Strength, ksi	Input Accel. of 1st Spalling	Displace. at 1st Spalling, in.	Max. Input Accel.*	Peak Force, Kips	Max. Displace. in*	Displace. Ductility*
Short	5.9	1.5g	1.3	1.95g	87.0	1.7	4.0
Medium	4.1	.75g	1.9	1.80g	50.0	6.4	6.0
Tall	4.11	0.9g	3.75	1.65g	33.4	10.0	8.0

* The maximum input acceleration, maximum displacement and displacement ductility are all based on a capacity equal to 80% of the peak capacity. Displacements are based on total system displacements.

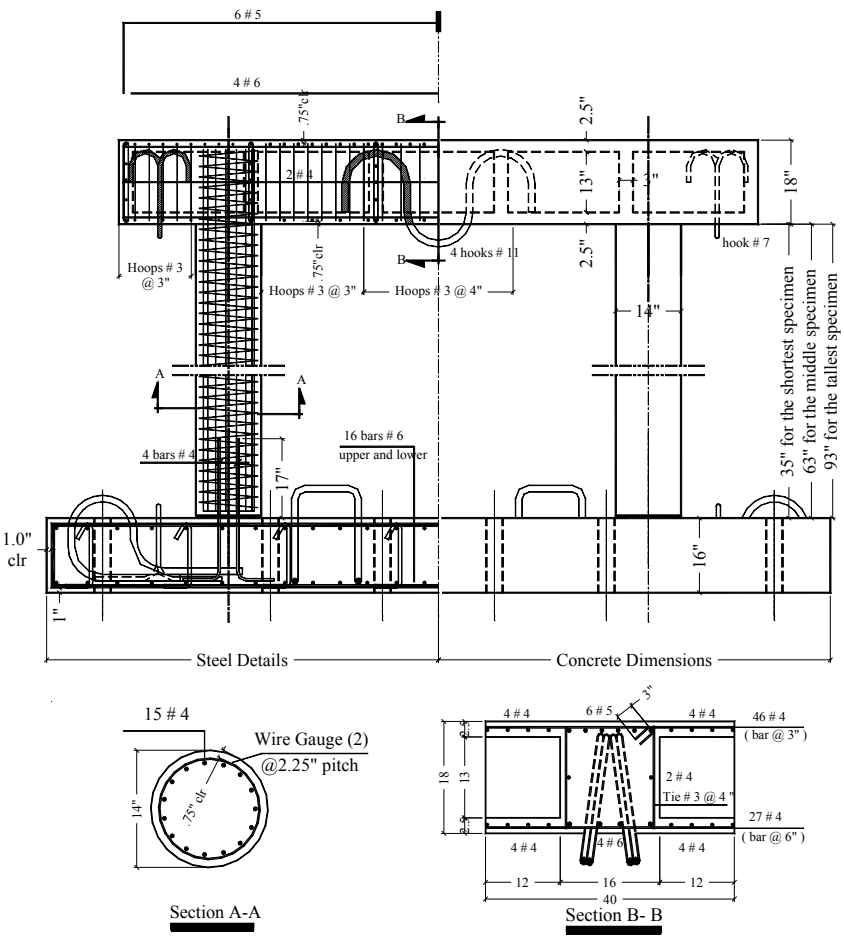

Fig. 1: Model Configuration

Fig. 2: Loading and Stability System

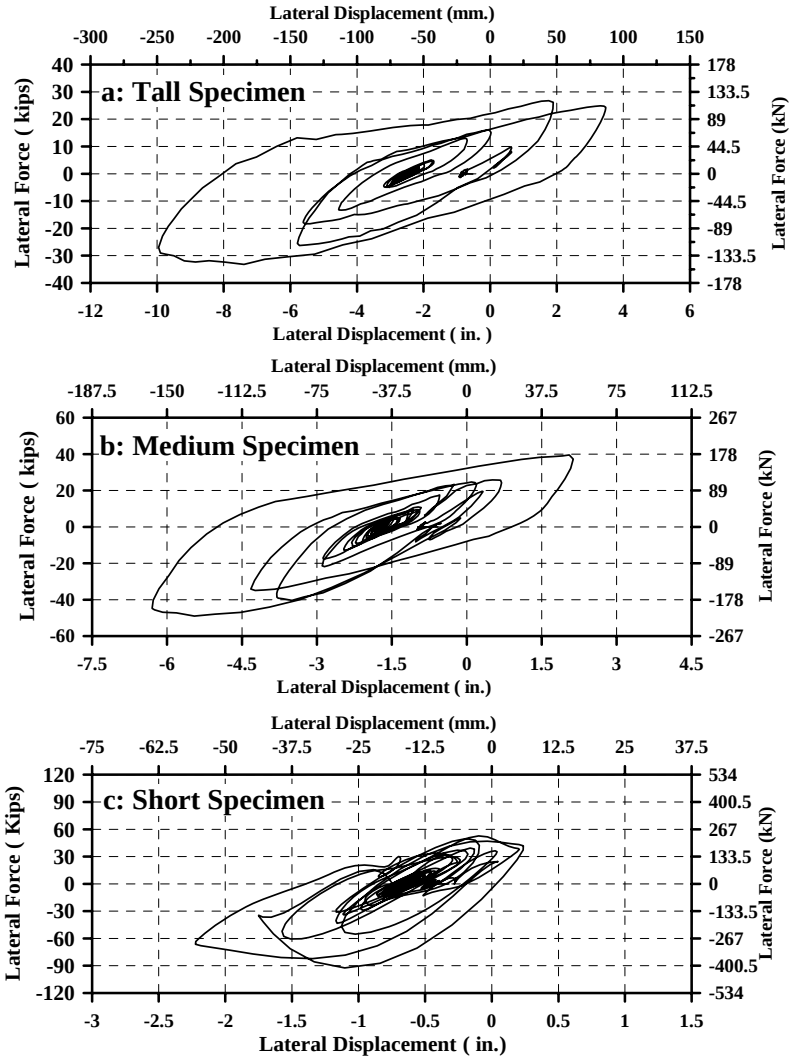

Fig. 3: Cumulative Experimental Hysteresis Responses for the Three Specimens

Fig. 4: Short Specimen (South-East View)

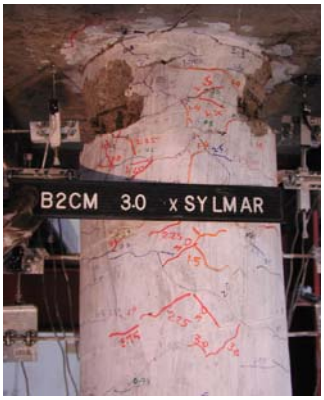

a) Hinge Base at West Column **b) West Column –South View**

Fig. 5: Observed Behavior in Medium Specimen

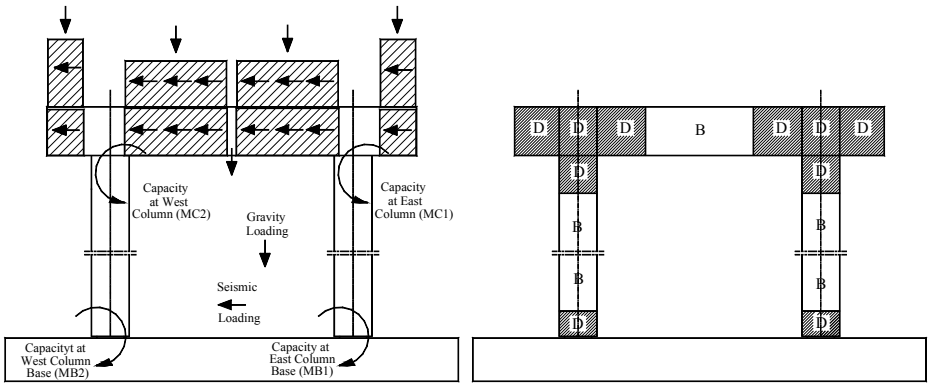

Fig. 6: Model Loading and Boundaries